Cancer Therapy: Preclinical

Clinical Cancer Research

The Anti-CD19 Antibody–Drug Conjugate SAR3419 Prevents Hematolymphoid Relapse Postinduction Therapy in Preclinical Models of Pediatric Acute Lymphoblastic Leukemia

Hernan Carol[1], Barbara Szymanska[1], Kathryn Evans[1], Ingrid Boehm[1], Peter J. Houghton[2], Malcolm A. Smith[3], and Richard B. Lock[1]

Abstract

Purpose: Relapsed or refractory pediatric acute lymphoblastic leukemia (ALL) remains a major cause of death from cancer in children. In this study, we evaluated the efficacy of SAR3419, an antibody–drug conjugate of the maytansinoid DM4 and a humanized anti-CD19 antibody, against B-cell precursor (BCP)-ALL and infant mixed lineage leukemia (MLL) xenografts.

Experimental Design: ALL xenografts were established as systemic disease in immunodeficient (NOD/SCID) mice from direct patient explants. SAR3419 was administered as a single agent and in combination with an induction-type regimen of vincristine/dexamethasone/L-asparaginase (VXL). Leukemia progression and response to treatment were assessed in real-time, and responses were evaluated using strict criteria modeled after the clinical setting.

Results: SAR3419 significantly delayed the progression of 4 of 4 $CD19^+$ BCP-ALL and 3 of 3 MLL-ALL xenografts, induced objective responses in all but one xenograft but was ineffective against T-lineage ALL xenografts. Relative surface CD19 expression across the xenograft panel significantly correlated with leukemia progression delay and objective response measure scores. SAR3419 also exerted significant efficacy against chemoresistant BCP-ALL xenografts over a large (10-fold) dose range and significantly enhanced VXL-induced leukemia progression delay in two highly chemoresistant xenografts by up to 82 days. When administered as protracted therapy following remission induction with VXL, SAR3419 prevented disease recurrence into hematolymphoid and other major organs with the notable exception of central nervous system involvement.

Conclusion: These results suggest that incorporation of SAR3419 into remission induction protocols may improve the outcome for high-risk pediatric and adult $CD19^+$ ALL. *Clin Cancer Res; 19(7); 1795–805.* ©*2013 AACR.*

Introduction

Acute lymphoblastic leukemia (ALL) is the most common childhood malignancy, constituting approximately 80% of pediatric leukemias and nearly one third of all childhood cancers (1). Over the past 50 years, advances in the treatment of pediatric ALLs have resulted in cure rates increasing from <10% to around 90% (2, 3). This improvement in patient outcome has principally resulted from the development of combination chemotherapy protocols, intensification of treatment for high-risk patients, and improvements in supportive care, rather than through the introduction of new drugs. Current induction treatment protocols, which use vincristine, a glucocorticoid and L-asparaginase (L-ASNase) with or without an anthracycline, result in >97% complete remission (CR) rates. Patients who relapse often exhibit multidrug resistance, which limits subsequent treatment options and contributes to poor outcome. In addition, ALL subtypes associated with specific chromosomal translocations, such as Philadelphia chromosome positive (Ph^+) ALL (t9;22) or those involving the mixed lineage leukemia (MLL) oncogene, remain particularly difficult to cure (4). While the incorporation of tyrosine kinase inhibitors into therapy for patients with Ph^+-ALLs has resulted in improved outcomes, the prognosis remains dismal for the majority of relapsed/refractory patients (2).

Monoclonal antibodies (mAb), and their toxin or drug conjugates, constitute a unique class of therapeutics that are

Authors' Affiliations: [1]Children's Cancer Institute Australia for Medical Research, University of New South Wales, Sydney, Australia; [2]Nationwide Children's Hospital, Columbus, Ohio; and [3]Cancer Therapy Evaluation Program, NCI, Bethesda, Maryland

Note: Supplementary data for this article are available at Clinical Cancer Research Online (http://clincancerres.aacrjournals.org/).

Corresponding Author: Richard B. Lock, Children's Cancer Institute Australia, Lowy Cancer Research Centre, UNSW, NSW 2052, Australia. Phone: 612-9385-2513; Fax: 612-9662-6583; E-mail: rlock@ccia.unsw.edu.au

doi: 10.1158/1078-0432.CCR-12-3613

Translational Relevance

Antibody–drug conjugates (ADC) are being used increasingly for cancer treatment. However, limited preclinical information is available on how best to combine ADCs with conventional chemotherapy. SAR3419 is a maytansinoid DM4/anti-CD19 ADC currently in clinical trials for the treatment of CD19-positive adult malignancies. Here, we report the results of preclinical studies in which SAR3419 was combined with a three-drug regimen (VXL) that mimics the induction treatment of pediatric patients with acute lymphoblastic leukemia (ALL) using well-characterized xenograft models of aggressive and chemoresistant ALLs. SAR3419 alone significantly delayed the progression of xenografts and elicited objective responses modeled after the clinical setting, the extent of which correlated with cell surface CD19 expression. However, the most profound effects were observed following remission induction with VXL, where SAR3419 prevented disease recurrence into hematolymphoid and other major organs. These results have significant implications for the combined use of established chemotherapy and SAR3419 in the treatment of relapsed/refractory ALLs.

particularly attractive as cancer treatments due to their antigen specificity and the effector/cytotoxic functions they can trigger. Advances in recombinant DNA technology led to the development of chimeric or humanized mAbs with reduced immunogenicity, thus overcoming a major complication associated with their clinical application. A growing number of antibody-based treatments are being approved for use by the U.S. Food and Drug Administration, many of these for cancer indications, including hematologic malignancies (reviewed in refs. 5, 6).

CD19 is a B-cell restricted co-receptor molecule expressed at high levels at all stages of B-cell differentiation except for mature plasma cells. As CD19 constitutes an important component of the B-cell receptor complex involved in signaling and antigen processing (7) and is expressed in the majority of B-cell precursor (BCP)-ALLs and B-cell non–Hodgkin lymphomas (NHL; ref. 8), it has long been recognized as a possible target in these malignancies. In the early 1990s, anti-CD19 antibodies conjugated to the blocked ricin toxin (9), pokeweed antiviral protein (10), and genistein (11) showed evidence of efficacy in preclinical studies. However, the initial clinical trials involving these agents were disappointing (12–14). Since then a new generation of anti-CD19 antibody–drug conjugates (ADC) have been developed, which are currently at various stages of preclinical and clinical evaluation (15–17). Also, the bispecific anti-CD19/anti-CD3 chimeric construct blinatumomab has shown promising results in a phase II clinical trial, further validating this target (18).

Maytansine is a potent antimitotic agent, which binds to tubulin and inhibits microtubule dynamics similar to *Vinca* alkaloids but with over 100-fold higher potency (19). Because of high toxicity and a small therapeutic index, its clinical development was halted (20). Interest in maytansine, and the 2 derived maytansinoids, DM1 and DM4, has recently been revived in the context of targeted delivery of drugs, which should minimize their toxicity (21, 22). Some of these agents such as trastuzumab emtansine (T-DM1), a DM1-ADC targeting the Her2 receptor in breast cancer, are advanced in their clinical development (23, 24). Other DM1 or DM4 ADCs are currently in preclinical and clinical development (25–28).

The principal objective of the Pediatric Preclinical Testing Program (PPTP) is to identify novel agents with significant antitumor activity against preclinical xenograft models of childhood solid tumors and ALL in immunodeficient mice and to prioritize the advancement of drugs into clinical trials. SAR3419 is an anti-CD19 humanized mAb (huB4) conjugated to DM4 (17, 29) currently tested in phase I/II clinical trials in relapsed or refractory B-cell NHL (NCT00539682 and NCT00549185) and adult ALL (NCT01440179; refs. 30, 31). In this study, we describe PPTP preclinical evaluation of SAR3419 and show that it is effective as a single-agent over a wide range of doses against $CD19^+$ BCP-ALL and MLL-ALL xenografts. More importantly, we show that when used as continuous treatment following remission induction with an induction-type regimen consisting of a combination of vincristine, the glucocorticoid dexamethasone (DEX) and L-ASNase (VXL), SAR3419 effectively prevented hematolymphoid relapse with mice succumbing to morbidity associated with central nervous system (CNS) relapse. Overall our data suggest that SAR3419 is a highly effective novel therapeutic agent for ALL and its incorporation into treatment protocols may improve the outcome for high-risk pediatric and adult patients with $CD19^+$ ALLs.

Materials and Methods

Xenograft models of pediatric ALL

All experimental studies were approved by the Animal Care and Ethics Committee of the University of New South Wales (New South Wales, Australia). The establishment and characterization of a pediatric patient-derived ALL xenograft panel in NOD/SCID (NOD.CB17-*Prkdc*^{scid}/J) mice has been previously described (refs. 32, 33; details can also be obtained from http://pptp.nchresearch.org/documents.html) and that of an infant MLL-rearranged xenograft panel will be published elsewhere. Mice obtained from Australian BioResources were inoculated intravenously with 2.5×10^6 to 5×10^6 ALL or MLL-ALL xenograft cells purified from spleens of previously engrafted mice. Leukemia engraftment was monitored by flow cytometric quantification of the proportion of human CD45-positive ($huCD45^+$) cells versus total $CD45^+$ leukocytes (human + murine) cells in the peripheral blood (PB) and tissues as described previously (32, 33). When the median %$huCD45^+$ cells in the PB was above 1% for each xenograft cohort, mice were randomized and allocated to groups (6–10 mice per group) and treatments initiated.

In vivo drug treatments

All drugs were administered by intraperitoneal injection (i.p.). Unless otherwise specified, drug schedules were as follows: SAR3419 1–10 mg/kg and huB4 10 mg/kg (provided by Sanofi, through the Cancer Therapy Evaluation Program, NCI) once a week for 3 weeks; vincristine (Baxter) 0.15 mg/kg once a week for 2 weeks; DEX (Sigma-Aldrich) 5 mg/kg, and L-ASNase (Leunase, Sanofi) 1,000 U/kg, Monday to Friday for 2 weeks. In some experiments, to prevent morbidity due to the immediate hypersensitivity reaction induced by MAb treatment, a pretreatment similar to standard clinical practice was administered 30 minutes before SAR3419. This prophylaxis consisted of acetaminophen (ref. 34; 100 mg/kg, Bristol-Myers Squibb) and promethazine (ref. 35; 4 mg/kg, Hospira) in a 0.2 mol/L NaCl/4 mg/mL glucose solution, i.p.

Determination of *in vivo* treatment response

An in-depth description of the analysis methods is included in the Summary Statistics and Analysis Methods section in Supplementary Material. Briefly, ALL xenograft responses to drug treatments were assessed using 2 activity measures, leukemia growth delay (LGD) and objective response measure (ORM) as previously described (36). Event-free survival (EFS) was calculated for each mouse as the number of days from treatment initiation until the %huCD45$^+$ cells in the PB reached 25% or until mice reached a humane endpoint with evidence of leukemia-related morbidity. EFS values for the different treatments were compared by Kaplan–Meier survival curves and log-rank test. The LGD was calculated for each group as the difference in median EFS between treated and control mice.

Each mouse was assigned an ORM score from 0 (progressive disease type 1, PD1) to 10 (maintained complete response, MCR), depending on its response profile (37), from which an overall response for the cohort was determined as the median ORM. According to this model, the following responses were defined during the 42-day monitoring period: progressive disease (PD) as a continuous increase in %huCD45$^+$ in the PB that reached event; stable disease (SD) as %huCD45$^+$ in the PB that did not decrease below 1% and did not reach event; partial response (PR) as a decrease of %huCD45$^+$ in the PB to under 1% at only one time point; complete response (CR) when the %huCD45$^+$ in the PB remained under 1% for 2 consecutive measures; and MCR when the %huCD45$^+$ in the PB stayed under 1% for the last 3 weeks of the monitoring period, or at 6 weeks from treatment initiation if monitoring extended beyond this time point. PD was further subdivided into the classifications PD1 or PD2 based on whether the EFS of the treated mouse was $\leq$1.5- or >1.5-fold, respectively, that of the median EFS of the control group. Median ORMs of PR, CR, and MCR were considered to be objective responses.

Responses were also expressed in a "COMPARE-like" format, which combines EFS and median ORMs around the midpoint (0) representative of SD. Bars to the right or left of the midpoint represent objective responses or nonobjective responses, respectively. Significant and nonsignificant differences in EFS distribution between control and treated cohorts are represented by red or blue color, respectively. Xenografts were excluded from analysis if >25% of mice within any one cohort experienced non–leukemia-related toxicity or morbidity.

CD19 expression analysis

RNA was extracted from cryopreserved xenograft cells harvested from spleens of highly engrafted animals (enriched by differential density centrifugation on Ficoll) using TRIzol (Sigma) and/or affinity purification spin columns (RNeasy, Qiagen). High-quality RNA (500 ng, verified using RNA 6000 LabChip kits and an Agilent 2100 Bioanalyzer) was amplified and cRNA was biotinylated using the Illumina TotalPrep RNA Amplification Kit (Ambion) as recommended by the manufacturer. Gene expression profiling was conducted using the Illumina Human Ref-12 Expression BeadChip (Illumina Inc.). Data from individual arrays were subjected to quantile normalization, and heatmaps were generated using the Heatmap Viewer module of GenePattern (38). Expression levels were normalized for each gene, where the mean is 0. Expression levels greater than the mean are shown in red and less than the mean are in blue as a logarithmic scale. Increasing distance from the mean is represented by increasing color intensity.

Relative surface expression of CD19 was evaluated by flow cytometry of xenograft cells obtained from both spleens and bone marrows of highly engrafted mice. For each xenograft, 3 independent samples were assessed. Samples were co-stained for huCD45$^+$ (allophycocyanin, APC-conjugated anti-human CD45, Biolegend) and CD19$^+$ (phycoerythrin, PE-conjugated anti-human CD19, BD Biosciences) and the mononuclear cell population within the leukocyte region (forward vs. side scatter plot) gated. For comparison purposes, unstained and PE-stained beads were included in each sample, and the geometric mean of the fluorescence intensity of the human population was normalized to both the corresponding signals of the unstained (RFI = 1) and stained beads (RFI = 100). Results are expressed as relative fluorescence intensity (RFI).

Histological detection of leukemia infiltration

Tissues were fixed in buffered formalin, dehydrated, cleared, and paraffin-embedded as per standard protocols. Sections (5 μm) were rehydrated and stained with hematoxylin and eosin and images obtained with bright field ScanScope slide scanning equipment and analyzed with ImageScope software (Aperio).

Statistical methods

The exact log-rank test as implemented using Proc StatXact for SAS was used to compare EFS distributions between treatment and control groups (2-tailed), with $P \leq 0.05$ considered significant. Correlations between CD19 mRNA or surface expression levels and LGD or ORM were analyzed using Spearman correlation test. For comparison of relative CD19 surface expression between spleen and bone marrow samples, a paired 2-tailed nonparametric test was applied.

Results

SAR3419 is highly effective as a single agent against CD19$^+$ ALL xenografts *in vivo*

The efficacy of SAR3419 as a single agent was first examined against a panel of 10 xenografts *in vivo* (5 BCP-ALL, 2 T-ALL, and 3 infant MLL-ALL). Treatments consisted of 3 injections administered once a week i.p. at a dose of 10 mg/kg. Compared with vehicle controls, SAR3419 significantly prolonged the EFS of all evaluable BCP-ALL and MLL-ALL xenografts (Fig. 1A–D, Table 1). For these xenografts,

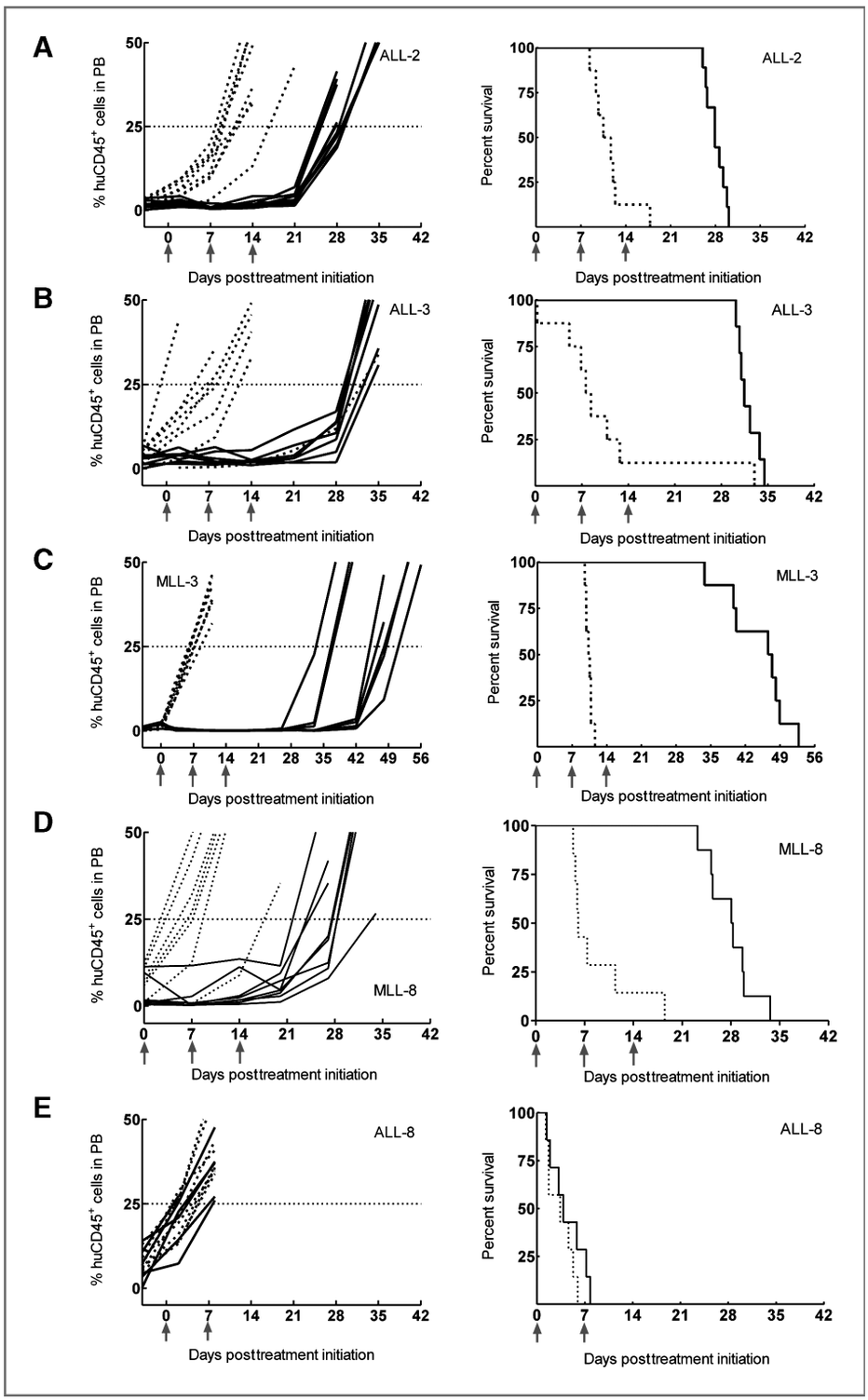

Figure 1. SAR3419 exerts significant *in vivo* single-agent efficacy against B-lineage pediatric ALL xenografts. NOD/SCID mice were inoculated with cells from BCP-ALL xenografts ALL-2 (A) and ALL-3 (B), infant MLL-ALL MLL-3 (C) and MLL-8 (D) or T-ALL ALL-8 (E). Following establishment of disease, mice were randomized and treated with vehicle (dashed lines) or 10 mg/kg SAR3419 (solid lines) once a week for 3 weeks. Response to treatment was monitored by weekly enumeration of the %huCD45$^+$ cells in the PB of individual mice (left); corresponding Kaplan–Meier curves (based on EFS) are shown on the right. Gray arrows indicate treatment times.

Table 1. Summary of xenografts and their *in vivo* responses to single-agent SAR3419

	Median EFS, d				
Xenograft	**Control**	**SAR3419**	**LGD, d**	***P*[a]**	**Median ORM**
BCP-ALL					
ALL-2	11.1	27.9	16.8	<**0.001**	PR
ALL-3	8.0	31.5	23.5	**0.0125**	PD2
ALL-4[b]	8.8	45.8	37.0	<**0.001**	CR
ALL-19	7.9	68.8	60.9	<**0.001**	CR
T-ALL					
ALL-8	3.4	3.5	0.1	0.466	PD1
ALL-16	11.6	21.0	9.4	0.580	PD2
Infant MLL-ALL					
MLL-3	10.5	47	36.5	<**0.001**	CR
MLL-8	7.0	28.2	21.2	<**0.001**	PR
MLL-14	7.0	37.6	30.6	<**0.001**	n.e.

NOTE: Of the 10 xenografts tested, ALL-17 is not included in this table due to toxicity greater than 25%.

Abbreviation: n.e., not evaluable for ORM response measure.

[a]Statistically significant differences are in bold.

[b]ALL-4 is a Ph^+ xenograft.

the LGDs ranged from 16.8 days for ALL-2 to 60.9 days for ALL-19 (Table 1). As expected, SAR3419 was ineffective in significantly delaying the progression of the 2 T-ALL xenografts (Fig. 1E, Table 1 and Supplementary Fig. S1A), which lack CD19 expression (32). SAR3419 elicited objective responses in 3 of 4 evaluable BCP-ALL xenografts (1 PR, 2CRs) and 2 of 2 evaluable MLL-ALL xenografts (1 PR, 1 CR; Table 1, Fig. 2A). In contrast, one of the most chemosensitive BCP-ALL xenografts in the panel (ALL-3; ref. 33) only achieved a PD2, and both T-ALL xenografts were scored as PD (1 PD1, 1 PD2). Xenograft responses to SAR3419 are also summarized in a "COMPARE-like" plot (Fig. 2B). A complete summary of results is provided in Supplementary Table S1, including total numbers of mice, number of mice that died (or were otherwise excluded), numbers of mice with events and average times to events, LGD values, as well as numbers of responses and T/C values. One BCP-ALL xenograft (ALL-17) was excluded from analysis due to toxicity; of the remaining 5 mice in the ALL-17 SAR3419-treated cohort 3 achieved CR, 1 PR, and 1 PD1 (Supplementary Fig. S1B). The xenograft MLL-14 was not evaluable in terms of ORM as due to its engraftment kinetics treatments commenced before the median leukemia load in PB was over 1% (Supplementary Fig. S1C).

In vivo efficacy of SAR3419 correlates with CD19 mRNA and cell surface expression

Microarray analysis of gene expression confirmed relatively high CD19 mRNA expression in BCP-ALL and MLL-ALL xenografts compared with T-lineage xenografts (Fig. 3A). These differences in relative expression were corroborated by flow cytometric analysis of cell surface CD19 expression (Fig. 3B and Supplementary Table S2). CD19 mRNA and cell surface protein expression in spleen-derived cells significantly correlated across 6 xenografts analyzed ($P < 0.001$, $R^2 = 0.98$, data not shown). Furthermore, CD19 mRNA expression correlated with *in vivo* responses to SAR3419 assessed by either median ORMs or LGD values of the xenografts tested (Fig. 3C). Overall, surface CD19 expression was significantly higher in xenograft cells collected from the bone marrow than in cells collected from the spleen ($P = 0.004$, Fig. 3C and Supplementary Table S2). Nevertheless, relative CD19 surface expression on cells collected from either anatomical site showed positive correlations with both the median ORMs and LGD values elicited by SAR3419 treatment (Fig. 3C).

SAR3419 exerts single-agent efficacy over a broad range of doses, whereas the unconjugated antibody is relatively ineffective

To further characterize the efficacy of SAR3419, a dose–response study was conducted against 2 $CD19^+$, chemoresistant xenografts, ALL-4 (Ph^+-ALL) and ALL-19, derived from patients who succumbed early to their disease (33). SAR3419 was highly efficacious against ALL-4, resulting in CRs for all doses tested (2.5–10 mg/kg, Fig. 2C and D, Table 2 and Supplementary Fig. S2A). A dose–response relationship was evident when the efficacy of SAR3419 was quantified by LGDs, which ranged from 22.3 to 36.8 days for 2.5 and 10 mg/kg doses, respectively (Supplementary Fig. S2A and Table 2). To further delineate the therapeutic window of SAR3419, we tested its efficacy at only 1 mg/kg against ALL-19. Even at this much reduced dose SAR3419 treatment elicited an ORM of SD in ALL-19, resulting in an LGD of 18.1 days (Fig. 2C and D, Table 2 and Supplementary Fig. S2B).

We also assessed the contribution of the DM4 drug component to the efficacy of this ADC, by comparing the effect of

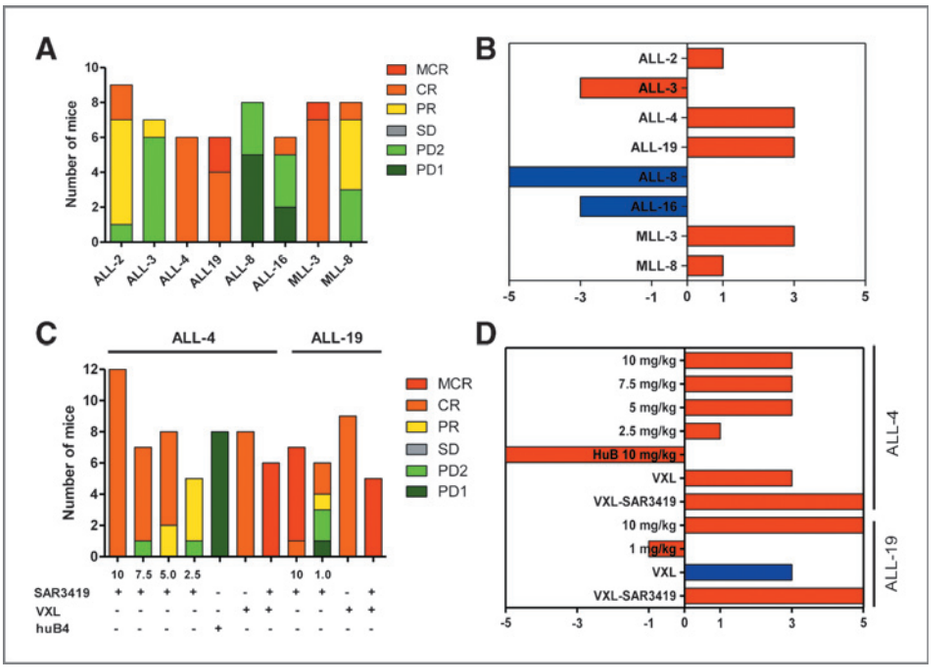

Figure 2. Summary of SAR3419 single-agent efficacy, dose–response, and VXL combination efficacy studies against pediatric ALL xenografts. A, distribution of ORMs of individual mice engrafted with BCP-ALL or infant MLL-ALL xenografts and treated with 10 mg/kg SAR3419 as described in Fig. 1. B, COMPARE-like plot of the midpoint difference representing the median ORM of xenografts shown in A. C, distribution of median ORMs of individual mice engrafted with ALL-4 or ALL-19 and treated with SAR3419 at different doses, mAb huB4, VXL, or VXL followed by SAR3419. D, COMPARE-like plot of the midpoint difference representing the median ORM of xenografts of xenografts shown in C. For the COMPARE-like plots in B and D, a score of −5 to 0 indicates that an objective response was not achieved for a particular xenograft, whereas a score of >0 to 5 indicates an objective response. Red bars indicate that the EFS was significantly different between control and treated mice. Blue bars indicate no significant difference.

SAR3419 to its unconjugated humanized MAb counterpart, huB4. At the same dose (10 mg/kg), huB4 only moderately (albeit significantly) delayed the progression of ALL-4 (Fig. 2C and D, Table 2 and Supplementary Fig. 2A) or ALL-19 (data not shown), but did not elicit an objective response, indicating that DM4 is critical for the high efficacy of SAR3419 against ALL in this xenograft experimental model.

SAR3419 prevents hematolymphoid relapse postremission induction

Our next aim was to assess whether SAR3419 could delay leukemia relapse postinduction therapy with established drugs. We have previously optimized, based on pharmacokinetic and tolerability parameters, an experimental induction–type protocol in NOD/SCID mice consisting of a VXL treatment platform (39). Mice engrafted with ALL-4 or ALL-19 were treated with VXL for 2 weeks to induce remission, followed immediately by one 3-week cycle of SAR3419 treatment with or without an ensuing 10-week block of weekly SAR3419 treatments at 10 mg/kg. VXL alone delayed the progression of both xenografts, by 18.0 days for ALL-4 (Fig. 4A and B, Table 2) and by 25.1 days for ALL-19 (Fig. 4C and D, Table 2) and resulted in objective responses (CRs) for both xenografts (Fig. 2C and D, Table 2).

The additional treatment with a 3-week cycle of SAR3419 following VXL significantly extended disease remission by 46.7 days for ALL-4 ($P = 0.0003$, Fig. 4A and B, Table 2) and by 82.3 days for ALL-19 ($P = 0.005$, Fig. 4C and D, Table 2) compared with VXL alone and resulted in therapeutic enhancement for both xenografts (Fig. 2C and D, Table 2). The effects of the VXL/SAR3419 combination were greater than additive for ALL-4 by 9.9 days and for ALL-19 by 21.4 days. All mice treated with one 3-week cycle of SAR3419 post-VXL eventually reached leukemia-related events (as defined by 25% huCD45$^+$ in PB) and exhibited high leukemic infiltration of all major organs (Fig. 4E and F).

Cohorts of mice engrafted with ALL-4 or ALL-19 also received an additional 10 weekly doses of SAR3419 treatment following the "VXL-SAR3419 × 3" regimen. This protracted SAR3419 treatment (VXL-SAR3419 × 13) also extended the disease remission induced by VXL alone for both xenografts and further extended the remission for ALL-4 in comparison with that obtained by the 3-week cycle of SAR3419 post-VXL schedule (Fig. 4, Table 2). However, all mice in the extended treatment cohorts eventually became morbid and were euthanized with undetectable levels of leukemic cells in the PB (Fig. 4E and F). Examination of tissues at necropsy revealed negligible leukemic infiltration of all major organs except for the brain and spinal fluid, as assessed by flow cytometry (Fig. 4E and F). The disparity in leukemic infiltration of spleen, bone marrow and brain, detected by flow cytometry, following either 3-week or prolonged SAR3419 administration post-VXL treatment was confirmed by histology (Supplementary Fig. S3).

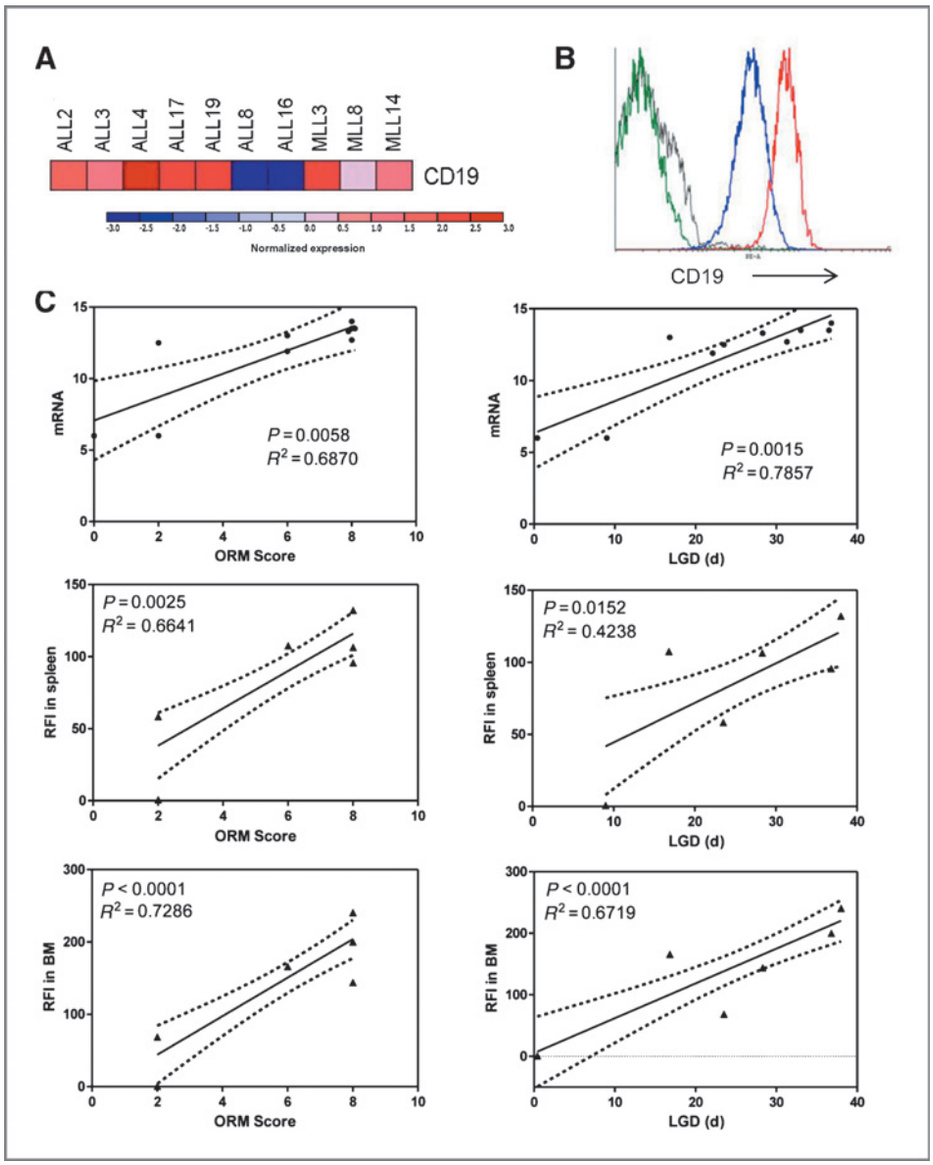

Figure 3. CD19 expression correlates with *in vivo* response to SAR3419. A, CD19 gene expression expressed in heatmap format (normalized to the mean, with relative expression depicted in logarithmic scale). B, representation of CD19 surface expression on three different xenografts (gray, isotype control; green, ALL-16; blue, ALL-3; red, ALL-19) as detected by flow cytometry. C, regression curves and 95% confidence intervals of CD19 mRNA in spleen-derived cells (top), and protein expression on cells derived from spleen (middle) or bone marrow (BM; bottom) correlated with the median ORMs (left) and LGDs (right) of the corresponding xenografts.

To exclude the possibility that the morbidity observed in this experiment was due to cumulative toxicity caused by prolonged exposure to SAR3419, we conducted a long-term toxicity study consisting of 13 weekly injections of 10 mg/kg SAR3419 or huB4 (10 in addition to the original 3-week cycle) using nonengrafted NOD/SCID mice. No clear evidence of toxicity was recorded. Throughout the study, all mice appeared healthy and asymptomatic, with no appreciable weight loss, whereas hematologic and biochemical analyses of PB samples, as well as histologic examination of tissues, revealed no relevant abnormalities (data not shown).

Discussion

This study is the first to provide preclinical evidence of high-level *in vivo* efficacy of the anti-CD19 DM4-ADC, SAR3419, against BCP-ALL and infant MLL-ALL xenografts. SAR3419 exerted potent single-agent activity against highly chemoresistant leukemia xenografts, which include ALL subtypes that remain difficult to treat such as Ph^+-ALL (ALL-4) and infant MLL-ALL. SAR3419 ranks among the four most efficacious single agents tested to date by the PPTP against the ALL xenograft panel, of more than 25 novel drugs tested, together with PR-104, MLN8237, and topotecan (37). The efficacy of SAR3419 against ALL xenografts was directly related to CD19 expression levels, with negligible activity toward T-ALL xenografts, and there was no nonspecific cytotoxicity against $CD19^-$ cells *in vivo*. These data indicate that SAR3419 is highly specific in targeting $CD19^+$ BCP-ALL xenografts. The higher density of CD19 expression in the bone marrow, together with the density-dependent efficacy of SAR3419, raises the possibility that

Table 2. Summary of *in vivo* ALL-4 and ALL-19 responses to a broad range of SAR3419 doses, unconjugated huB4 mAb, and SAR3419 following VXL treatment

Xenograft	Treatment	Median EFS, d	LGD, days)	*P*	Median ORM[a]
ALL-4	Control (vehicle)	8.9			
	SAR3419 (10 mg/kg)	45.7	36.8	0.00016	CR
	SAR3419 (7.5 mg/kg)	39.2	30.3	<0.0001	CR
	SAR3419 (5 mg/kg)	34.4	25.5	<0.0001	CR
	SAR3419 (2.5 mg/kg)	31.2	22.3	0.0050	CR
	huB4 (10 mg/kg)	13	4.1	0.00226	PD1
	Control (vehicle)	10.1			
	VXL	28.1	18	<0.0001	CR
	VXL-SAR3419 × 3	74.8	64.7	0.0002	MCR
	VXL-SAR3419 × 13	91.5	81.4	0.0014	MCR
ALL-19	Control (vehicle)	7.9			
	SAR3419 (10 mg/kg)	68.8	60.9	0.00058	MCR
	SAR3419 (1 mg/kg)	26.0	18.1	0.00117	SD
	Control (vehicle)	8.3			
	VXL	33.4	25.1	0.06913	CR
	VXL-SAR3419 × 3	115.7	107.4	0.00126	MCR
	VXL-SAR3419 × 13	105.0	96.7	0.00833	MCR

[a]Assessed at 6 weeks from treatment initiation.

SAR3419 may target ALL xenograft cells residing in the bone marrow more effectively than those in the spleen or PB. Consistent with results from a lymphoma model study (17, 29), the unconjugated mAb had only minimal effect on the target cells indicating that DM4 is an essential component of this ADC responsible for its cytotoxic effect. Target-bound anti-CD19 antibodies (Ab) are reported to undergo fast internalization making them particularly suitable for targeted delivery of cytotoxic molecules to malignant cells while reducing off-target toxicity (29). Upon internalization, the ADC is degraded, releasing DM4 intracellularly, which binds to tubulin and disrupts microtubule assembly leading to apoptosis (29).

In a recent study using preclinical models of B-cell lymphoma *in vivo*, the efficacy of SAR3419 was shown to be comparable with that of chemotherapy and superior to that of rituximab (17) Although rituximab is capable of inducing apoptosis directly, its clinical efficacy appears largely dependent on complement-dependent cytotoxicity (CDC) and antibody-dependent cell-mediated cytotoxicity (ADCC), recruitment of effector cells and upregulation of cytokine secretion (40). The contributions of CDC and ADCC cannot be adequately assessed in the immunodeficient NOD/SCID mouse host used in this study, thereby precluding direct comparisons between SAR3419 and rituximab.

The relevance of CD19 as a target in B-lineage malignancies is highlighted by encouraging clinical trial results with blinatumomab (18). Historical preclinical studies using other anti-CD19 mAbs and their conjugates were encouraging, showing efficacy in preclinical models of B-cell leukemias and lymphomas (9, 10, 41). However, the ensuing clinical trials produced disappointing results (12, 42, 43). The reasons for these failures are likely to be multifactorial, including limited access of the ADCs to certain disease sites, excessive nonspecific toxicity associated with the conjugated toxin component, resistance to the drug used in the conjugate, and development of immunity against mouse Abs (HAMA). The humanized anti-CD19 Ab component of SAR3419 is expected to elicit minimal immune response, which should increase its therapeutic potential and allow for repeated use. Recent data from phase I/II clinical trials of SAR3419 in relapsed or refractory B-cell NHL were very encouraging (30, 31). SAR3419 is relatively safe with few toxic effects mainly associated with prolonged treatment; however, no significant myelosuppression was observed. There was strong evidence of single-agent activity; objective responses (CRs or PRs) were observed in 33% of patients with stage III or IV NHLs treated with SAR3419 at its maximum tolerated dose. Approximately 50% of patients exhibited more than 20% reduction in their tumor burden in response to SAR3419 at any dose (it is worth noting that approximately half of these patients had rituximab-resistant disease). These early results suggest that SAR3419 is a safe and effective agent against B-cell NHLs with a large therapeutic window. These findings are consistent with a previously reported study using lymphoma models (29) and data observed in this study where we show a large therapeutic window of efficacy. Of note, our mouse xenograft model is unable to assess the impact that this treatment may have on the normal human B lymphocyte compartment.

We have previously reported that ALL-4 and ALL-19 are relatively chemoresistant xenografts, exhibiting resistance

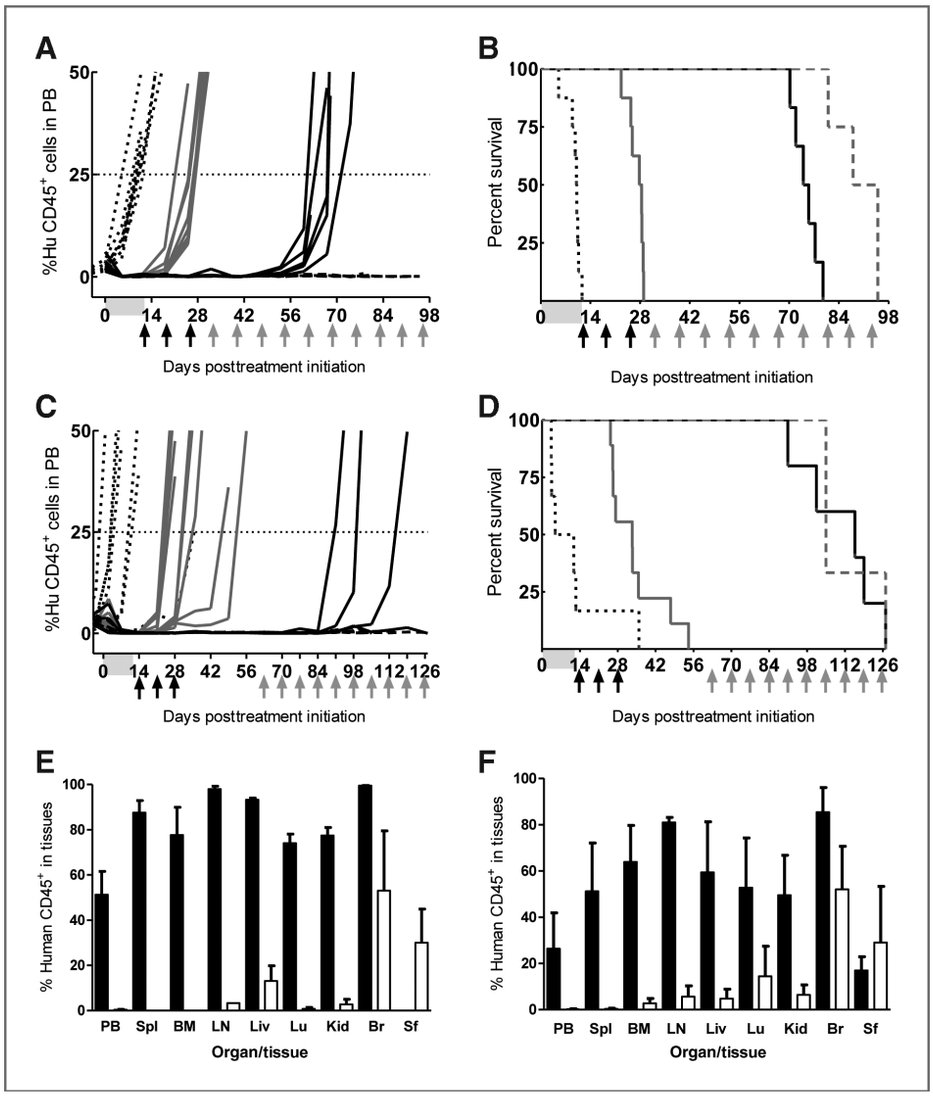

Figure 4. Efficacy of SAR3419 against BCP-ALL xenografts following remission induction with VXL therapy. Mice engrafted with ALL-4 (A, B, E), or ALL-19 (C, D, F), were treated with vehicle (black dotted lines); VXL (gray solid lines); VXL followed by 3 weekly doses of SAR3419 (black solid lines) or VXL followed by up to 13 weekly doses of SAR3419 (gray dashed lines). For additional details, see Materials and Methods. The VXL treatment period is indicated by the gray shading, and SAR3419 treatment time points are marked by black (×3) and gray arrows (×10). Left, the %huCD45$^+$ cells in PB of individual mice; right, Kaplan–Meier plots of EFS. Infiltration of %huCD45$^+$ cells (E and F) in various organs or tissues at necropsy: VXL/SAR3419 times 3 weeks (black bars), VXL/SAR3419 extended treatment (white bars). Br, brain; BM, bone marrow; LN, lymph node; Liv, liver; Lu, lung; Kid, kidney; Spl, spleen; SF, spinal fluid.

to a broad range of therapeutic agents including DEX, L-ASNase, rapamycin, sunitinib, and vorinostat (33, 37, 44). A critical finding of the current study is that a 3-week course of SAR3419 following VXL "induction" treatment significantly extended the length of remission and ORMs, whereas protracted SAR3419 post-VXL prevented relapse of leukemia into hematolymphoid tissues and other peripheral organs, except for the CNS. This observation may not be surprising, as in our experimental model, treatment begins when systemic disease is already well-established, and mAbs are known to be inefficient in penetrating the blood–brain barrier. Therefore, any residual disease within the CNS not eradicated with the VXL therapy is likely to cause relapse. In the long-term treatment experiments, mice became morbid with no evidence of leukemia in the PB, and as the SAR3419 preparation contains <1% of free DM4 (17, 29), it was conceivable that continuous exposure to low doses of DM4 may still induce toxicity. The long-term toxicity study conducted in nonengrafted mice revealed there were no obvious side effects caused by SAR3419 exposure, suggesting that the observed morbidity in leukemia-bearing mice was likely due to the invasion of the CNS by the leukemia. Although a study of lymphoma infiltration by tomography monitoring in a mouse model suggests that there may be a reduction in the lymphoma burden of the spinal canal following SAR3419 treatment (29), this may be insufficient to prevent CNS relapse in the long-term (17). Our results suggest that SAR3419 may be particularly effective in eliminating residual disease following remission induction with standard therapy that includes intrathecal methotrexate to prevent CNS relapse.

In conclusion, this study has shown the following: (i) SAR3419 is a highly potent and selective cytotoxic agent targeting BCP-ALL and infant MLL-ALL xenografts expressing cell surface CD19; (ii) SAR3419 has a large therapeutic window and minimal toxicity in a mouse xenograft model; (iii) when administered following an induction-type VXL regimen, SAR3419 induces durable remissions in highly

chemoresistant ALL xenografts; and (iv) when administered as maintenance therapy following VXL treatment, SAR3419 effectively prevents leukemia relapse in hematolymphoid and other major peripheral organs except for the CNS. Therefore, we provide strong preclinical evidence for the efficacy of SAR3419 against broadly chemoresistant pediatric BCP-ALL and infant MLL-ALL xenografts, which argues for its incorporation into existing therapies that could result in improved outcomes for pediatric and adult patients with otherwise poor prognosis.

Disclosure of Potential Conflicts of Interest

H. Carol has an ownership interest (including patents). Children's Cancer Institute Australia for Medical Research is affiliated with the University of New South Wales and the Sydney Children's Hospitals Network. No potential conflicts of interest were disclosed by the other authors.

Authors' Contributions

Conception and design: H. Carol, B. Szymanska, P.J. Houghton, M.A. Smith, R.B. Lock
Development of methodology: H. Carol, M.A. Smith, R.B. Lock
Acquisition of data (provided animals, acquired and managed patients, provided facilities, etc.): H. Carol, B. Szymanska, K. Evans, I. Boehm, R.B. Lock
Analysis and interpretation of data (e.g., statistical analysis, biostatistics, computational analysis): H. Carol, B. Szymanska, K. Evans, P.J. Houghton, M.A. Smith, R.B. Lock
Writing, review, and/or revision of the manuscript: H. Carol, B. Szymanska, K. Evans, P.J. Houghton, M.A. Smith, R.B. Lock
Administrative, technical, or material support (i.e., reporting or organizing data, constructing databases): B. Szymanska, K. Evans, I. Boehm, P.J. Houghton
Study supervision: H. Carol, R.B. Lock

Acknowledgments

The authors thank Laura High for assistance with gene expression analysis and Mila Dolotin for excellent technical assistance. The authors also thank Sanofi-Aventis for supplying SAR3419 and the huB4 antibody.

Grant Support

This study was supported by National Cancer Institute grant numbers: NOI-CM-42216 and NOI-CM-91001-03.

The costs of publication of this article were defrayed in part by the payment of page charges. This article must therefore be hereby marked *advertisement* in accordance with 18 U.S.C. Section 1734 solely to indicate this fact.

Received November 22, 2012; revised January 20, 2013; accepted February 10, 2013; published OnlineFirst February 20, 2013.

References

1. Kaatsch P. Epidemiology of childhood cancer. Cancer Treat Rev 2010;36:277–85.
2. Hunger SP, Raetz EA, Loh ML, Mullighan CG. Improving outcomes for high-risk ALL: translating new discoveries into clinical care. Pediatr Blood Cancer 2011;56:984–93.
3. Hunger SP, Lu X, Devidas M, Camitta BM, Gaynon PS, Winick NJ, et al. Improved survival for children and adolescents with acute lymphoblastic leukemia between 1990 and 2005: a report from the Children's Oncology Group. J Clin Oncol 2012;30:1663–9.
4. Pui CH, Carroll WL, Meshinchi S, Arceci RJ. Biology, risk stratification, and therapy of pediatric acute leukemias: an update. J Clin Oncol 2011;29:551–65.
5. Li Y, Zhu Z. Monoclonal antibody-based therapeutics for leukemia. Expert Opin Biol Ther 2007;7:319–30.
6. Scott AM, Wolchok JD, Old LJ. Antibody therapy of cancer. Nat Rev Cancer 2012;12:278–87.
7. Harwood NE, Batista FD. New insights into the early molecular events underlying B cell activation. Immunity 2008;28:609–19.
8. Uckun F, Jaszcz W, Ambrus J, Fauci AS, Gajl-Peczalska K, Song CW, et al. Detailed studies on expression and function of CD19 surface determinant by using B43 monoclonal antibody and the clinical potential of anti-CD19 immunotoxins. Blood 1988;71:13–29.
9. Shah SA, Halloran PM, Ferris CA, Levine BA, Bourret LA, Goldmacher VS, et al. Anti-B4-blocked ricin immunotoxin shows therapeutic efficacy in four different SCID mouse tumor models. Cancer Res 1993;53:1360–7.
10. Ek O, Gaynon P, Zeren T, Chelstrom LM, Myers DE, Uckun FM. Treatment of human B-cell precursor leukemia in SCID mice by using a combination of the anti-CD19 immunotoxin B43-PAP with the standard chemotherapeutic drugs vincristine, methylprednisolone, and L-asparaginase. Leuk Lymphoma 1998;31:143–9.
11. Uckun FM, Evans WE, Forsyth CJ, Waddick KG, Ahlgren LT, Chelstrom LM, et al. Biotherapy of B-cell precursor leukemia by targeting genistein to CD19-associated tyrosine kinases. Science 1995;267:886–91.
12. Multani PS, O'Day S, Nadler LM, Grossbard ML. Phase II clinical trial of bolus infusion anti-B4 blocked ricin immunoconjugate in patients with relapsed B-cell non-Hodgkin's lymphoma. Clin Cancer Res 1998;4:2599–604.
13. Szatrowski TP, Dodge RK, Reynolds C, Westbrook CA, Frankel SR, Sklar J, et al. Lineage specific treatment of adult patients with acute lymphoblastic leukemia in first remission with anti-B4-blocked ricin or high-dose cytarabine: Cancer and Leukemia Group B Study 9311. Cancer 2003;97:1471–80.
14. Morris JC, Waldmann TA. Antibody-based therapy of leukaemia. Expert Rev Mol Med 2009;11:e29.
15. Gerber HP, Kung-Sutherland M, Stone I, Morris-Tilden C, Miyamoto J, McCormick R, et al. Potent antitumor activity of the anti-CD19 auristatin antibody drug conjugate hBU12-vcMMAE against rituximab-sensitive and -resistant lymphomas. Blood 2009;113:4352–61.
16. Bernt KM, Prokop A, Huebener N, Gaedicke G, Wrasidlo W, Lode HN. Eradication of CD19+ leukemia by targeted calicheamicin. Bioconj Chem 2009;20:1587–94.
17. Al-Katib AM, Aboukameel A, Mohammad R, Bissery MC, Zuany-Amorim C. Superior antitumor activity of SAR3419 to rituximab in xenograft models for non-Hodgkin's lymphoma. Clin Cancer Res 2009;15:4038–45.
18. Topp MS, Gökbuget N, Zugmaier G, Degenhard E, Goebeler M-E, Klinger M, et al. Long-term follow-up of hematologic relapse-free survival in a phase 2 study of blinatumomab in patients with MRD in B-lineage ALL. Blood 2012;120:5185–7.
19. Remillard S, Rebhun LI, Howie GA, Kupchan SM. Antimitotic activity of the potent tumor inhibitor maytansine. Science 1975;189:1002–5.
20. Cassady JM, Chan KK, Floss HG, Leistner E. Recent developments in the maytansinoid antitumor agents. Chem Pharm Bull 2004;52:1–26.
21. Chari RV. Targeted cancer therapy: conferring specificity to cytotoxic drugs. Accounts Chem Res 2008;41:98–107.
22. Lopus M, Oroudjev E, Wilson L, Wilhelm S, Widdison W, Chari R, et al. Maytansine and cellular metabolites of antibody-maytansinoid conjugates strongly suppress microtubule dynamics by binding to microtubules. Mol Cancer Ther 2010;9:2689–99.
23. Blackwell KL, Miles D, Gianni L, Krop IE, Welslau M, Baselga J, et al. Primary results from EMILIA, a phase III study of trastuzumab emtansine (T-DM1) versus capecitabine (X) and lapatinib (L) in HER2-positive locally advanced or metastatic breast cancer (MBC) previously treated with trastuzumab (T) and a taxane. J Clin Oncol 30, 2012 (suppl; abstr LBA1).
24. Burris HA III, Rugo HS, Vukelja SJ, Vogel CL, Borson RA, Limentani S, et al. Phase II study of the antibody drug conjugate trastuzumab-DM1 for the treatment of human epidermal growth factor receptor 2 (HER2)-positive breast cancer after prior HER2-directed therapy. J Clin Oncol 2011;29:398–405.

25. Erickson HK, Park PU, Widdison WC, Kovtun YV, Garrett LM, Hoffman K, et al. Antibody-maytansinoid conjugates are activated in targeted cancer cells by lysosomal degradation and linker-dependent intracellular processing. Cancer Res 2006;66:4426–33.
26. Kovtun YV, Audette CA, Mayo MF, Jones GE, Doherty H, Maloney EK, et al. Antibody-maytansinoid conjugates designed to bypass multidrug resistance. Cancer Res 2010;70:2528–37.
27. Lapusan S, Vidriales M, Thomas X, de Botton S, Vekhoss A, Tang R, et al. Phase I studies of AVE9633, an anti-CD33 antibody-maytansinoid conjugate, in adult patients with relapsed/refractory acute myeloid leukemia. Invest New Drugs 2012;30:1121–31.
28. Oroudjev E, Lopus M, Wilson L, Audette C, Provenzano C, Erickson H, et al. Maytansinoid-antibody conjugates induce mitotic arrest by suppressing microtubule dynamic instability. Mol Cancer Ther 2010; 9:2700–13.
29. Blanc V, Bousseau A, Caron A, Carrez C, Lutz RJ, Lambert JM. SAR3419: an anti-CD19-maytansinoid immunoconjugate for the treatment of B-cell malignancies. Clin Cancer Res 2011;17 :6448–58.
30. Coiffier B, Ribrag V, Dupuis J, Tilly H, Haioun C, Morschhauser F, et al. Phase I/II study of the anti-CD19 maytansinoid immunoconjugate SAR3419 administered weekly to patients (pts) with relapsed/refractory B-cell non-Hodgkin lymphoma (NHL). ASCO Meeting Abstracts 2011;29:8017.
31. Younes A, Kim S, Romaguera J, Copeland A, Farial S, Kwak LW, et al. Phase I multidose-escalation study of the anti-CD19 maytansinoid immunoconjugate SAR3419 administered by intravenous infusion every 3 weeks to patients with relapsed/refractory B-cell lymphoma. J Clin Oncol 2012;30:2776–82.
32. Lock RB, Liem N, Farnsworth ML, Milross CG, Xue C, Tajbakhsh M, et al. The nonobese diabetic/severe combined immunodeficient (NOD/SCID) mouse model of childhood acute lymphoblastic leukemia reveals intrinsic differences in biologic characteristics at diagnosis and relapse. Blood 2002;99:4100–8.
33. Liem NL, Papa RA, Milross CG, Schmid MA, Tajbakhsh M, Choi S, et al. Characterization of childhood acute lymphoblastic leukemia xenograft models for the preclinical evaluation of new therapies. Blood 2004; 103:3905–14.
34. Miranda HF, Puig MM, Prieto JC, Pinardi G. Synergism between paracetamol and nonsteroidal anti-inflammatory drugs in experimental acute pain. Pain 2006;121:22–8.
35. Nascimento JEB, Costa KA, Bertollo CM, Oliveira ACP, Rocha LTS, Souza ALS, et al. Pharmacological investigation of the nociceptive response and edema induced by venom of the scorpion Tityus serrulatus. Toxicon 2005;45:585–93.
36. Houghton PJ, Morton CL, Tucker C, Payne D, Favours E, Cole C, et al. The pediatric preclinical testing program: Description of models and early testing results. Pediatr Blood Cancer 2007;49:928–40.
37. Szymanska B, Carol H, Lock RB. Preclinical evaluation. In:Saha V, Kearns P, eds. New agents for the treatment of acute lymphoblastic leukemia. Springer: New York; 2011. p. 39–60.
38. Reich M, Liefeld T, Gould J, Lerner J, Tamayo P, Mesirov JP. GenePattern 2.0. Nat Genet 2006;38:500–1.
39. Szymanska B, Wilczynska-Kalak U, Kang MH, Liem NLM, Carol H, Boehm I, et al. Pharmacokinetic modeling of an induction regimen for *in vivo* combined testing of novel drugs against pediatric acute lymphoblastic leukemia xenografts. PLoS One 2012;7:e33894.
40. Bezombes C, Fournie J-J, Laurent G. Direct effect of rituximab in B-cell-derived lymphoid neoplasias: mechanism, regulation, and perspectives. Mol Cancer Res 2011;9:1435–42.
41. Liu C, Lambert JM, Teicher BA, Blattler WA, O'Connor R. Cure of multidrug-resistant human B-cell lymphoma xenografts by combinations of anti-B4-blocked ricin and chemotherapeutic drugs. Blood 1996;87:3892–8.
42. Grossbard ML, Lambert JM, Goldmacher VS, Spector NL, Kinsella J, Eliseo L, et al. Anti-B4-blocked ricin: a phase I trial of 7-day continuous infusion in patients with B-cell neoplasms. J Clin Oncol 1993;11: 726–37.
43. Dinndorf P, Krailo M, Liu-Mares W, Frierdich S, Sondel P, Reaman G. Phase I trial of anti-B4-blocked ricin in pediatric patients with leukemia and lymphoma. J Immunother 2001;24:511–6.
44. High LM, Szymanska B, Wilczynska-Kalak U, Barber N, O'Brien R, Khaw SL, et al. The Bcl-2 homology domain 3 mimetic ABT-737 targets the apoptotic machinery in acute lymphoblastic leukemia resulting in synergistic in vitro and in vivo interactions with established drugs. Mol Pharmacol 2010;77:483–94.